

Theoretical Bounds on Time-Domain Resolution of Multilevel Carrier-Based Digital PWM Signals Used in All-Digital Transmitters

Tanovic, O.; Ma, R.; Teo, K.H.

TR2017-106 August 2017

Abstract

Pulse-width modulation (PWM) has been extensively used in switched converter systems, and recently in RF applications, due to an increased interest in all-digital transmitters. These architectures employ high efficiency switched-mode power amplifiers (SMPA), where PWM is commonly used to generate the PA driving signal. However, digitally implemented PWM introduces large amount of in-band distortion, which is traditionally explained by spectral aliasing. In this paper we derive a novel closed-form time-domain expression for the output signal of a multilevel carrier-based digital PWM, driven by an arbitrary bounded input signal. We show that the spectral aliasing effects are equivalent to amplitude quantization of the PWM input signal, and give theoretical bounds on the output signal resolution for a given PWM scheme. Parameters of this quantization process are determined, and their dependence on PWM design specifications is shown. Numerical simulations in MATLAB were used to verify derived analytical expressions.

IEEE International Midwest Symposium on Circuits and Systems

This work may not be copied or reproduced in whole or in part for any commercial purpose. Permission to copy in whole or in part without payment of fee is granted for nonprofit educational and research purposes provided that all such whole or partial copies include the following: a notice that such copying is by permission of Mitsubishi Electric Research Laboratories, Inc.; an acknowledgment of the authors and individual contributions to the work; and all applicable portions of the copyright notice. Copying, reproduction, or republishing for any other purpose shall require a license with payment of fee to Mitsubishi Electric Research Laboratories, Inc. All rights reserved.

Theoretical Bounds on Time-Domain Resolution of Multilevel Carrier-Based Digital PWM Signals Used in All-Digital Transmitters

Omer Tanovic*[†], Rui Ma* and Koon Hoo Teo*

Email: otanovic@mit.edu {rma, teo}@merl.com

* Mitsubishi Electric Research Laboratories, Cambridge, MA, USA,

[†] Laboratory for Information and Decision Systems, Department of Electrical Engineering and Computer Science, Massachusetts Institute of Technology, Cambridge, MA, USA,

Abstract—Pulse-width modulation (PWM) has been extensively used in switched converter systems, and recently in RF applications, due to an increased interest in all-digital transmitters. These architectures employ high efficiency switched-mode power amplifiers (SMPA), where PWM is commonly used to generate the PA driving signal. However, digitally implemented PWM introduces large amount of in-band distortion, which is traditionally explained by spectral aliasing. In this paper we derive a novel closed-form time-domain expression for the output signal of a multilevel carrier-based digital PWM, driven by an arbitrary bounded input signal. We show that the spectral aliasing effects are equivalent to amplitude quantization of the PWM input signal, and give theoretical bounds on the output signal resolution for a given PWM scheme. Parameters of this quantization process are determined, and their dependence on PWM design specifications is shown. Numerical simulations in MATLAB were used to verify derived analytical expressions.

I. INTRODUCTION

In recent years, RF power amplifiers in switched-mode operation (SMPA), have gained a lot of attention from researchers in microwave community, due to their high power efficiency mode of operation [1]-[2]. SMPAs are driven by multilevel signals, which are allowed to assume only certain discrete amplitude values. Baseband pulse-width modulation (PWM) is commonly used for reduction of amplitude resolution, of e.g. I or Q baseband signal components (or their amplitude, in burst-mode transmitters [2]), to adjust for switched-mode operation. PWM maps an input signal into a digital pulse train, where amplitude information of the input is encoded into time-varying width of the output pulses [3]-[5]. PWM has been traditionally implemented in analog domain, and we denote such modulation scheme as analog PWM. Forthcoming communication standards envision transceivers implemented as software-defined radio [1], utilizing available signal processing power in digital domain. In this setup, PWM is fully digitally implemented (both input and output of PWM are digital signals), and is best described as a 'time sampled' version of its analog counterpart. Sampling of an infinite bandwidth analog PWM signal leads to spectral aliasing, producing considerable amount of distortion in the digital PWM output's frequency band of interest. This represents the main drawback of digitally

implemented PWM. Spectral aliasing effects in digital PWM have been studied in the past through simple frequency domain analysis and numerical simulation [6]-[7], and different algorithms were proposed for mitigating this distortion in all-digital transmitter (ADT) architectures (e.g. see [8] and references therein). Finite time resolution of switching instants in digital PWM signals implies finite resolution of the output pulse widths, and correspondingly of the input signal amplitude. In the past this has been studied and exploited only in two-level PWM schemes for switched converter systems (e.g. [9]).

In this paper we derive a novel closed-form time-domain expression for the output signal of a multilevel carrier-based digital PWM, driven by an arbitrary bounded input signal. We show that the spectral aliasing effects are equivalent to amplitude quantization of the PWM input signal, and give theoretical bounds on the achievable signal resolution, as well as dependence of the quantization process on the choice of PWM parameters. This result implies that aliasing-free digital PWM is possible if and only if the PWM input signal is pre-quantized exactly as defined by the inherent quantization process. We give derivations for symmetric double-edge PWM only, but explain why analysis extends to arbitrary choice of carrier signals. The presented analysis significantly improves understanding of the leading in-band distortion source in digitally implemented PWM, and represents fundamental step in understanding behavior and limits of ADT architectures employing PWM.

II. ANALYTICAL MODEL OF PWM

In this paper we consider carrier-based (CB) double-edge (DE) amplitude-slicing multilevel (ML) PWM system [5], and refer to it simply as PWM in the following sections.

A. Analog PWM

In carrier-based PWM schemes, output signal is generated by comparing input to a fixed carrier signal (e.g. sawtooth or sinusoid), as shown in Fig.1. So let $c = c(t)$ be a symmetric double-edge sawtooth signal, oscillating between 0 and 1 with frequency f_p . Signal $c(t)$ is used as a baseline to generate contiguous carriers in multilevel PWM operation. Frequency f_p is then called the carrier of pulse frequency of PWM, and $T_p = 1/f_p$ is the carrier period).

This work was done while Omer Tanovic was an intern at Mitsubishi Electric Research Laboratories (MERL).

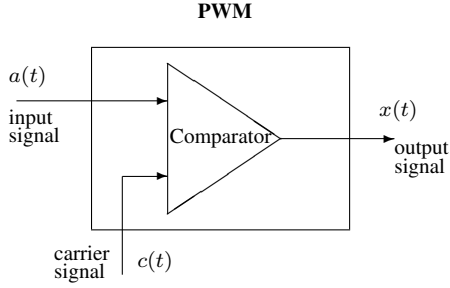


Fig. 1. Block diagram describing basic operation of PWM.

In the case of $(M + 1)$ -level PWM (corresponding to M carriers), contiguous carriers $c_m(t)$ can be expressed in terms of $c(t)$ as follows:

$$c_m(t) = \frac{1}{M}c(t + \tau) + \frac{m-1}{M}, \quad m = 1, \dots, M$$

where $\tau = T_p/2$ if m is odd, and $\tau = 0$ otherwise. PWM input signal $a(t)$ is assumed to be a bounded signal, taking values in the interval $(0, 1)$. PWM output signal $x(t)$ is then generated by comparing $a(t)$ and $c_m(t)$ as follows:

$$x(t) = \begin{cases} 1, & c_M(t) \leq a(t) < 1, \\ \frac{m}{M}, & c_m(t) \leq a(t) < c_{m+1}(t), 1 \leq m \leq M-1, \\ 0, & 0 < a(t) < c_1(t) \end{cases} \quad (1)$$

An example of output signal generation in a three-level PWM scheme is illustrated in Fig.2. In this case $M = 2$, and output signal $x(t)$ assumes values 0, 1/2 or 1.

In the rest of this paper, we will use \mathbf{P} to denote a PWM operator with an arbitrary (but fixed) number of output levels, where the actual number should be clear from the context. Using double Fourier series and the fact that $c(t)$ is periodic, signal $x(t)$ can be expressed (see e.g. [10]) as

$$x(t) = (\mathbf{P}a)(t) = a(t) + \sum_{k=1}^{\infty} \frac{2 \sin(\pi M k a(t))}{\pi M k} \cos(2k\pi f_p t). \quad (2)$$

The above expression can be rewritten as

$$x(t) = x_0(t) + \sum_{k=1}^{\infty} x_k(t) \cos(2k\pi f_p t), \quad (3)$$

where

$$x_0(t) = a(t), \quad x_k(t) = \frac{2 \sin(\pi M k a(t))}{\pi M k}, \quad \forall k \in \mathbb{N}. \quad (4)$$

It follows that $x(t)$ can be described as a sum of the baseband component $x_0(t)$, equal to the input $a(t)$, and amplitude modulated harmonics $x_k(t)$ at integer multiples of the PWM carrier frequency f_p . Therefore $x(t)$ is of infinite bandwidth.

B. Digital PWM

The operation of digital PWM can be defined in a similar way. For given $T_s > 0$, let $\tilde{c} = \tilde{c}[n] = c(nT_s)$ be the discrete-time (DT) symmetric double-edge sawtooth carrier signal, obtained from $c(t)$ by sampling at rate $1/T_s$. Given

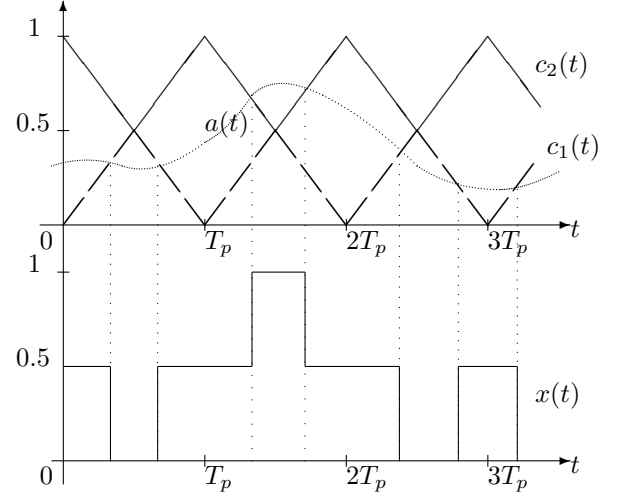


Fig. 2. An example of output signal generation in three-level analog PWM.

$\tilde{c}[n]$, an $(M + 1)$ -level digital PWM operator maps bounded real-valued input signal \tilde{a} into output signal \tilde{x} , as given below

$$\tilde{x}[n] = \begin{cases} 1, & \tilde{c}_M[n] \leq \tilde{a}[n] < 1, \\ \frac{m}{M}, & \tilde{c}_m[n] \leq \tilde{a}[n] < \tilde{c}_{m+1}[n], 1 \leq m \leq M-1, \\ 0, & 0 < \tilde{a}[n] < \tilde{c}_1[n] \end{cases} \quad (5)$$

where contiguous DT carriers $\tilde{c}_m[n]$ are obtained from $c_m(t)$ by sampling at rate $1/T_s$. In the next section we use the above definition of digital PWM to find an expression for $\tilde{x}[n]$ in terms of $\tilde{a}[n]$, similar to that in (2) for $x(t)$ and $a(t)$.

III. TIME-DOMAIN ANALYSIS OF DIGITAL PWM

In this section we consider digital PWM system with carrier frequency f_p and $(M + 1)$ output levels. Let $f_s = N \cdot f_p$ and $T_s = \frac{1}{f_s}$ be the sampling frequency and sampling period respectively, where $N > 1$ is the oversampling ratio of PWM. Without loss of generality we assume N to be an integer, which is true in most practical applications. We also assume that N is odd, since analysis in the case of even N is almost identical.

Let (\tilde{a}, \tilde{x}) be an input-output signal pair of a digital PWM system, that is $\tilde{x} = \mathbf{P}\tilde{a}$ holds, and let analog signal $a(t)$, with $0 < a(t) < 1, \forall t \in \mathbb{R}$, be such that $\tilde{a}[n] = a(nT_s)$. It now follows from (2) and (5) that signal \tilde{x} can be expressed as

$$\begin{aligned} \tilde{x}[n] &= a(nT_s) + \sum_{k=1}^{\infty} \frac{2 \sin(\pi M k a(nT_s))}{\pi M k} \cos(2k\pi f_p nT_s) \\ &= \tilde{a}[n] + \sum_{k=1}^{\infty} \frac{2 \sin(\pi M k \tilde{a}[n])}{\pi M k} \cos\left(\frac{2\pi}{N} kn\right). \end{aligned}$$

The above sum is an infinite sum, but the number of possibly different harmonics is finite, and equal to N . Furthermore, signal \tilde{x} is real-valued, so its Fourier transform is conjugate symmetric, and the number of independent harmonics is equal to $(\lfloor \frac{N}{2} \rfloor + 1)$. It follows that signal \tilde{x} can be expressed as

$$\tilde{x}[n] = \tilde{x}_0[n] + \sum_{k=1}^{\lfloor \frac{N}{2} \rfloor} \tilde{x}_k[n] \cos\left(\frac{2\pi}{N} kn\right), \quad (6)$$

where

$$\begin{aligned}\tilde{x}_0[n] &= \tilde{a}[n] + 2 \cdot \sum_{l=1}^{\infty} \frac{\sin(\pi MNl\tilde{a}[n])}{\pi MNl}, \\ \tilde{x}_k[n] &= 2 \cdot \sum_{l=0}^{\infty} \frac{\sin(\pi M(Nl+k)\tilde{a}[n])}{\pi M(Nl+k)} + \\ &+ 2 \cdot \sum_{l=0}^{\infty} \frac{\sin(\pi M(Nl+N-k)\tilde{a}[n])}{\pi M(Nl+N-k)},\end{aligned}\quad (7)$$

with $1 \leq k \leq \lfloor \frac{N}{2} \rfloor$. Here \tilde{x}_0 denotes the baseband component of \tilde{x} , and \tilde{x}_k are higher order harmonics, similar to the description of analog PWM output, given in (3). It is clear that aliasing effects manifest in (7) in terms of an infinite number of additional summands. Let us now simplify expressions in (7). Baseband component \tilde{x}_0 can be rewritten as

$$\tilde{x}_0[n] = \tilde{a}[n] + \sum_{l=1}^{\infty} \frac{\sin(\pi MNl\tilde{a}[n])}{\pi MNl} + \sum_{l=-\infty}^{-1} \frac{\sin(\pi MNl\tilde{a}[n])}{\pi MNl}.$$

Since $\left. \frac{\sin(\pi MNl\tilde{a}[n])}{\pi MNl} \right|_{l=0} = \tilde{a}[n]$, we get

$$\tilde{x}_0[n] = \sum_{l=-\infty}^{\infty} \frac{\sin(\pi MNl\tilde{a}[n])}{\pi MNl}. \quad (8)$$

Similarly, by applying change of variables in the second equality in (7), expression for \tilde{x}_k simplifies to

$$\tilde{x}_k[n] = 2 \cdot \sum_{l=-\infty}^{\infty} \frac{\sin(\pi M(Nl+k)\tilde{a}[n])}{\pi M(Nl+k)}, \quad 1 \leq k \leq \left\lfloor \frac{N}{2} \right\rfloor. \quad (9)$$

It can be observed from (8) and (9) that expressions for harmonics of \tilde{x} involve only infinite sums of discrete sinc functions which can be computed analytically (see Appendix).

Let \mathbf{Q} be a uniform quantizer with dynamic range $(0, 1)$ and $L = \lfloor \frac{MN}{2} \rfloor$ output levels, and let \tilde{a}_Q denote the response of \mathbf{Q} to signal \tilde{a} , i.e. $\tilde{a}_Q[n] = (\mathbf{Q}\tilde{a})[n]$. From (8), (9) and results given in the Appendix, it follows that

$$\begin{aligned}\tilde{x}_0[n] &= \tilde{a}_Q[n], \\ \tilde{x}_k[n] &= \frac{2 \sin(\pi k M \tilde{a}_Q[n])}{MN \sin(\frac{\pi k}{N})}, \quad 1 \leq k \leq \left\lfloor \frac{N}{2} \right\rfloor.\end{aligned}\quad (10)$$

Thus, a DT analog of CT equation (2) can be written as

$$\tilde{x}[n] = \tilde{a}_Q[n] + \sum_{k=1}^{\lfloor \frac{N}{2} \rfloor} \frac{2 \sin(\pi k M \tilde{a}_Q[n])}{MN \sin(\frac{\pi k}{N})} \cos\left(\frac{2\pi}{N}kn\right). \quad (11)$$

PWM output is by definition a pulsed signal (whose Fourier series coefficients are sinc functions) and therefore a formula similar to (11) should hold, regardless of the choice of baseline carrier. Though parameters of the quantization process may change in this case, e.g. for trailing edge PWM $L = MN$ holds, and for sinusoidal carriers quantization process would be non-uniform. Expression (11) now implies that aliasing-free digital PWM is possible if and only if the PWM input signal is pre-quantized exactly as defined by the inherent quantization process. In order to minimize in-band distortion introduced by the inherent quantization, e.g. delta-sigma modulator (DSM) can be used to pre-quantize digital PWM input, and shape

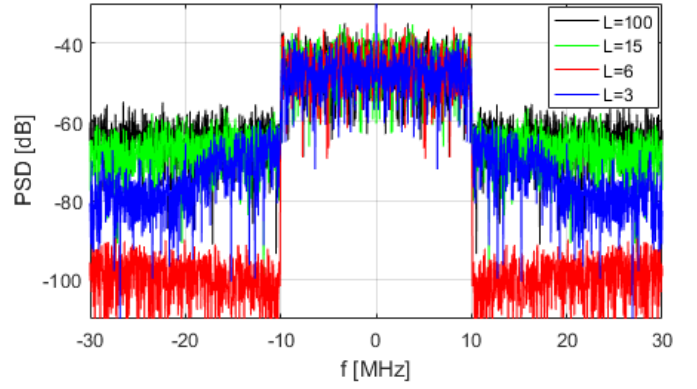


Fig. 3. Baseband spectrum of digital PWM output for different number of DSM pre-quantization levels.

noise to out-of-band frequencies. But relation $L = \lfloor \frac{MN}{2} \rfloor$ is crucial in achieving optimal in-band signal-to-noise ratio (SNR). Indeed, if it is not satisfied, additional in-band distortion will be generated by PWM, as confirmed by Matlab simulation results shown in Fig. 3. These plots depict baseband spectrum of the output of a digital PWM with $M = 2$ and $N = 6$, driven by the same high resolution input signal with four different DSM configurations: uniformly quantized with the number of quantization levels L equal to 100, 15, 6 and 3. Clearly $L = 6$ satisfies relation $L = \lfloor \frac{MN}{2} \rfloor$, and gives optimal in-band SNR.

IV. MODEL VERIFICATION

In order to verify the closed-form expressions derived in the previous section, numerical simulations in MATLAB have been carried. Amplitude of a randomly generated 64QAM signal, upsampled and rescaled in amplitude to fit into $(0, 1)$ interval, has been used as the input into digital PWM. Input signal bandwidth is set to $B = 20$ MHz, and the PWM carrier frequency is $f_p = 0.5$ GHz. Both the oversampling ratio N and the number of output levels $(M + 1)$ of PWM have been varied. Relative distance between digital PWM output signals obtained by simulation of a process shown in Fig. 1. and by the derived analytical formulas, was used as a measure of error. That is, if x and x_a denote PWM outputs obtained by numerical simulation and analytical formulas, respectively, the error is given as

$$d(x, x_a) = \frac{\|x - x_a\|_2}{\|x\|_2} \cdot 100 \quad [\%] \quad (12)$$

Values of (12), for various combinations of N and M , are shown in Table I. As can be seen, the error is negligible, which confirms validity of derived expressions. As an illustration the spectra of a digital PWM output signal obtained by simulation, and the corresponding validation error signal, for $N = 4$ and $M = 4$, are shown in Fig. 4. It is clear that power level of the error signal, between simulated and analytically obtained PWM outputs, is significantly lower than the signal level, as was expected from error values in Table I.

V. CONCLUSION

In this paper, a novel closed-form time-domain expression for the output signal of a multilevel carrier-based digital

TABLE I. DIFFERENCE BETWEEN SIMULATED AND ANALYTICALLY OBTAINED DIGITAL PWM OUTPUT (VALUES IN PART-PER-TRILLION OF %)

$\frac{M+1}{N}$	3	5	7	9	11	13
2	0	0	0.001	0	0.001	0.001
3	0.197	0.164	0.120	0.090	0.076	0.063
4	0.108	0.074	0.053	0.041	0.034	0.028
5	0.158	0.120	0.086	0.067	0.055	0.045
6	0.323	0.224	0.159	0.125	0.103	0.085
7	0.201	0.150	0.111	0.085	0.069	0.057
8	0.202	0.139	0.097	0.077	0.062	0.051
9	0.349	0.249	0.179	0.140	0.114	0.094
10	0.247	0.172	0.120	0.094	0.077	0.064

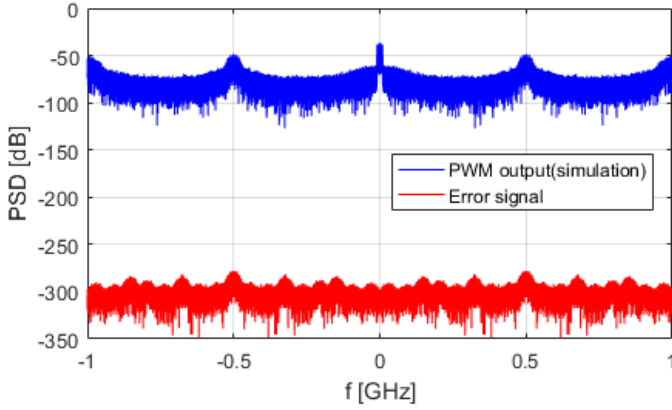


Fig. 4. Spectra of simulated digital PWM output and error signals.

PWM, driven by an arbitrary bounded input signal, was presented. Quantization process, due to finite time resolution of switching instants inherent to digital PWM operation, was fully described, giving theoretical bounds on the achievable output signal resolution for a given PWM scheme. It was shown that this quantization is a time-domain manifestation of spectral aliasing effects in digital PWM. This result implies that aliasing-free digital PWM is possible if and only if the input signal, before being fed into PWM, is quantized exactly as defined by the inherent quantization process. The presented analysis significantly improves understanding of the leading in-band distortion source in digitally implemented PWM.

APPENDIX

We find closed form expressions for infinite sums in (8) and (9) by sampling carefully chosen continuous-time signals, and then use the Fourier transform to compute the DC component.

For fixed $a \in (0, 1)$, let continuous-time signal f be defined as $f(t) = \frac{\sin(\pi at)}{\pi t}$ for $t \neq 0$ and $f(0) = a$. The Fourier transform of signal f is given by

$$F(\omega) = \begin{cases} 1, & |\omega| < \pi a \\ 0, & \text{otherwise} \end{cases}.$$

Let $S(K, a) = \sum_{n=-\infty}^{\infty} \frac{\sin(\pi Kna)}{\pi Kn}$. Clearly the infinite sum in (8) is equal to $S(K, a)$ for $K = MN$. For $T > 0$, let discrete-time signal f_T be defined as

$$f_T[n] = f(nT) = \frac{\sin(\pi anT)}{\pi nT}, \quad \forall n \in \mathbb{Z}.$$

The sum $S(K, a)$ can now be rewritten in terms of f_T as

$$S(K, a) = \sum_{n=-\infty}^{\infty} f_T[n] \Big|_{T=K}.$$

Let F_T denote the Fourier transform of f_T . Since f_T is a sampled version of f , F_T is given as

$$F_T(\Omega) = \frac{1}{T} \sum_{k=-\infty}^{\infty} F\left(\frac{\Omega}{T} - \frac{2\pi k}{T}\right). \quad (13)$$

Evaluating F_T at $\Omega = 0$ we get $F_T(0) = \sum_{n=-\infty}^{\infty} f_T[n]$, and hence

$$S(K, a) = F_T(0) \Big|_{T=K}. \quad (14)$$

Thus computing $S(K, a)$ amounts to finding the value of F_T at $\Omega = 0$. From (13) and (14) it follows that

$$S(K, a) = \frac{1}{K} \sum_{k=-\infty}^{\infty} F\left(-\frac{2\pi k}{K}\right). \quad (15)$$

Depending on the values of K and a , the number of elements in the sum in (15) will change. More precisely

$$F\left(-\frac{2\pi k}{K}\right) = 1 \text{ for } \left| \frac{2\pi k}{K} \right| \leq \pi a,$$

which implies

$$S(K, a) = \frac{2\mu + 1}{K}, \quad (16)$$

where $\mu = \lfloor \frac{aK}{2} \rfloor$. This can be restated as follows

$$S(K, a) = \frac{2k + 1}{K}, \quad (17)$$

where $\frac{2k}{K} \leq a < \frac{2k+2}{K}, \forall k \in \{0, \dots, \lfloor \frac{K-1}{2} \rfloor\}$.

Infinite sum in (9) can be found in a similar way by sampling function $g(t) = f(t + Mk)$ for $1 \leq k \leq \lfloor \frac{N}{2} \rfloor$.

REFERENCES

- [1] F. Ghannouchi, "Power Amplifier and Transmitter Architectures for Software Defined Radio Systems," *IEEE Circuits Syst. Mag.*, vol. 10, no. 4, pp. 56-63, Nov. 2010.
- [2] B. Francois, E. Kaymaksut, and P. Reynaert, "Burst mode operation as an efficiency enhancement technique for RF power amplifiers," in *Proc. GA Scientific Symp. Int. Union Radio Sci.*, Aug. 2011, pp. 14.
- [3] H. Black, *Modulation Theory*, Van Nostrand, 1953.
- [4] F. H. Raab, "Radio frequency pulsewidth modulation," *IEEE Trans. Commun.*, vol. COM-21, no. 8, pp. 958-966, Aug. 1973.
- [5] G. Carrara, S. Gardella, M. Marchesoni, R. Salutati and G. Sciuotto, "A new multilevel PWM method: A theoretical analysis," *IEEE Trans. Power Electron.*, vol. 7, no. 3, pp. 497-505, Jul. 1992.
- [6] S. Santi, R. Rovatti, and G. Setti, "Spectral aliasing effects of PWM signals with time-quantized switching instants," in *Proc. 2004 Int. Symp. Circuits Syst. (ISCAS2004)*, pp. 689-692, May 2004.
- [7] A. Amin, M. El-Korfolly and S. Mohammed, "Exploring aliasing distortion effects on regularly-sampled PWM signals," in *Proc. 3rd IEEE Conf. Ind. Electron. Appl.*, pp. 2036-2041, Jun. 2008.
- [8] K. Hausmair, S. Chi, P. Singerl and C. Vogel, "Aliasing-Free Digital Pulse-Width Modulation for Burst-Mode RF Transmitters," *IEEE Trans. Circuits Syst. I, Reg. Papers*, vol. 60, no. 2, pp. 415-427, Feb. 2013.
- [9] M. Norris, L. M. Platon, E. Alarcon, and D. Maksimovic, "Quantization Noise Shaping in Digital PWM Converters," presented at the *120th Audio Engineering Soc. Conv.*, pp. 127-133, Rhodes, Jun. 2008.
- [10] H. Enzinger and C. Vogel, "Analytical description of multilevel carrier-based PWM of arbitrary bounded input signals," in *Proc. 2014 Int. Symp. Circuits Syst. (ISCAS2014)*, pp. 1030-1033, Melbourne VIC, Jun. 2014.